Int. J. Multiphase Flow Vol. 11, No. 3, pp. 269–281, 1985
Printed in the U.S.A.

0301-9322/85 $3.00 + .00

STUDIES ON HEAT TRANSFER AND FLOW CHARACTERISTICS IN SUBCOOLED FLOW BOILING—PART 1. BOILING CHARACTERISTICS

RYUTARO HINO† and TATSUHIRO UEDA‡
Department of Mechanical Engineering, University of Tokyo, Bunkyo-ku, Tokyo 113, Japan

(*Received* 5 *June* 1984; *in revised form* 29 *October* 1984)

Abstract—Measurement of wall temperature profile and photographic observation are performed for R-113 subcooled boiling flow in a channel with heat fluxes up to the CHF. The incipient boiling superheats measured are little affected by mass velocity and liquid subcooling. Hysteresis in boiling observed by increasing and decreasing heat flux seems to be ascribed to variation in size of active nucleation cavities on the wall. Increasing heat flux up to the CHF, the bubble density on the heated surface increases and remarkably large coalescent bubbles appear periodically near the heating section outlet.

1. INTRODUCTION

The liquid supplied to flow boiling channels is usually in a subcooled state. In such systems, the first heat transfer process encountered is that of convective heat transfer to single-phase liquid, and the nucleate boiling is initiated at some position along the heated length where the wall temperature exceeds the saturation value. The bulk liquid temperature at this position is generally less than the saturation value. The boiling process up to a point where the core liquid reaches the saturation temperature is called subcooled boiling.

From a viewpoint of the flow state, the subcooled boiling flow is divided into two regions. One is referred to the high subcooling region (region I) where bubbles remain attached to or slide along the heated surface. The other is referred to the low subcooling region (region II) where bubbles grow and disperse in the liquid core and the void fraction increases sharply with the heating length. The point at which the void fraction starts to rise sharply, i.e. the transition point to the region II, is called the point of net vapor generation. On the other hand, taking note of the heat transfer characteristics, the subcooled boiling process is divided into the partial nucleate boiling and the fully developed nucleate boiling, and the critical heat flux (CHF) condition in the subcooled boiling flow may occur at a high heat flux.

These characteristics of subcooled boiling flow have been investigated to a considerable extent. As for the conditions of incipient boiling, Sato & Matsumura (1964), Bergles & Rohsenow (1964) and Davis & Anderson (1966) proposed analytical models based on the presence of available cavities on the heated surface. Levy (1967), Staub (1968), Saha & Zuber (1974), Sekoguchi *et al.* (1974) and Dougall & Lippert (1971) proposed criteria for the point of net vapor generation. Clark & Rohsenow (1954) and Bergles & Rohsenow (1964) presented heat transfer correlations for both regions of partial and fully developed nucleate boiling. Murphy & Bergles (1972) and Abdelmessih *et al.* (1974) have observed the boiling curve hysteresis caused by variation in size of active cavities on the heating surface.

However, since the subcooled boiling flow is in a complicated nonequilibrium state involving the vapor bubbles and the subcooled liquid, the subcooled boiling process is not yet clarified in detail. The present study was undertaken to obtain some information about the heat transfer to subcooled boiling flow and the state of bubbles flowing close to the heated surface. In this paper, the experimental results of heat transfer characteristics for R-113

†Present address: Division of High Temperature Engineering, Japan Atomic Energy Research Institute, Tokai, Naka-Gun, Ibaragi-Prefecture 319-11, Japan.
‡Present address: Department of Mechanical Engineering, Kogakuin University, 1, Nishishinjuku, Shinjuku-ku, Tokyo 160, Japan.

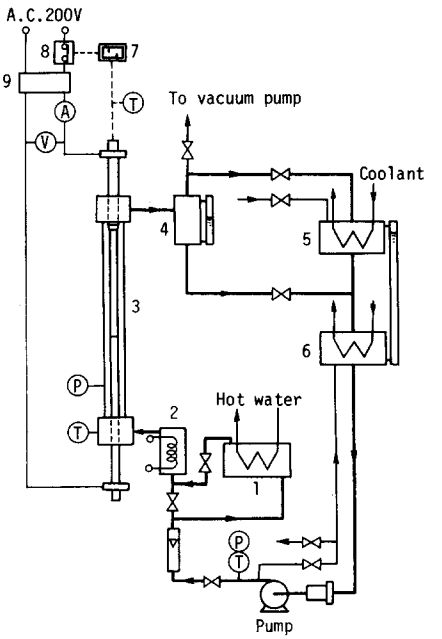

Figure 1. Flow diagram of experimental apparatus. 1. Preheater, 2. Control heater, 3. Test section, 4. Liquid–vapor separator, 5. Condenser, 6. Storage tank, 7. 8. Excess temperature trip, 9. Voltage regulator and transformer.

subcooled boiling flow are presented comparing with the photographic observation of the flow state.

2. APPARATUS AND PROCEDURE

A flow diagram of the apparatus is shown in figure 1. Fluorocarbon R-113 liquid in a storage tank is supplied by a circulating pump to the test section at a fixed subcooling through a preheater and a control heater, and flows upwards in the annular passage. Vapor generated in the test section is separated by a separator connected to the outlet end of the test section and led to a condenser.

The test section is a vertically arranged concentric annulus with an inner tube heated. The inner tube is composed of a heating section and copper electrodes silver-soldered to both ends of the heating section. The heating section, a stainless-steel tube of 8 mm o.d., 0.5 mm thick and 400 mm long, is heated uniformly by passing an alternating current through it. The outer tube is made of a pyrex tube of 18 mm i.d., so that the hydraulic diameter D_e is 10 mm. The length of the annular passage is 800 mm, and that of the entrance region to the heating section is 380 mm. The surface of heating section was finished with No. 4/0 emerypaper. Four movable C–A thermocouples were arranged axially inside the heating section. The junctions of these thermocouples were press fitted onto the inner surface by Teflon plugs inserted into the heating section. The outer surface temperature T_w of the heating section was then derived from the measured inner surface temperature taking into account heat conduction in the tube wall with heat generation.

In the experiments, the pressure at the test section inlet was kept at a fixed value p_{in} = 0.147 MPa (the corresponding saturation temperature being 332 K). The experimental ranges covered are

$$\text{Mass velocity} \quad G = 158\text{–}1600 \text{ kg/m}^2 \text{ s},$$

$$\text{Inlet subcooling} \quad \Delta T_{sub} = T_s - T_{Lin} = 10\text{–}30 \text{ K}.$$

Measurement of the wall temperature distribution along the heating section and photo-

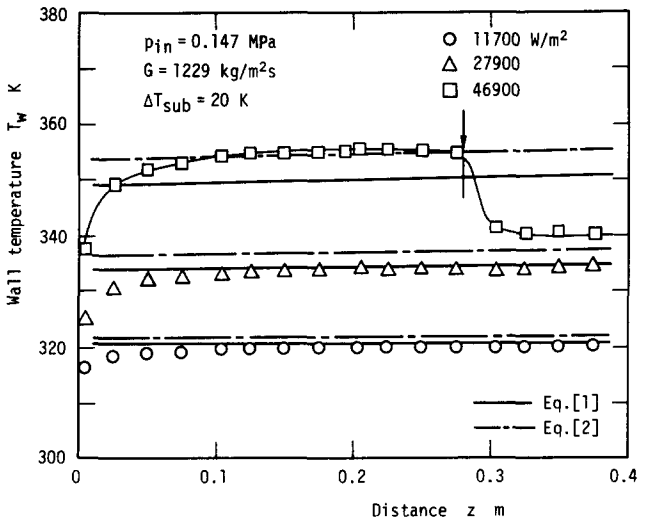

Figure 2. Wall temperature profiles.

graphic observation on the state of bubble generation were performed in a range of heat fluxes up to the CHF.

3. INCIPIENT BOILING AND BOILING CURVE HYSTERESIS

3.1 *Incipient boiling*

Figures 2 and 3 show the wall temperature distributions along the heating length z obtained at an inlet subcooling ΔT_{sub} = 20 K. As is seen in these figures, when the wall superheat required for incipient boiling is realized with increasing heat flux, the nucleate boiling initiates near the heating section outlet. Arrows drawn in these figures indicate the position where bubbles were first observed. The wall temperature drops sharply near the position and becomes approximately constant in the downstream region of nucleate boiling. The position of incipient boiling shifts upstream with increasing heat flux.

The straight lines shown in these figures represent the wall temperature calculated from

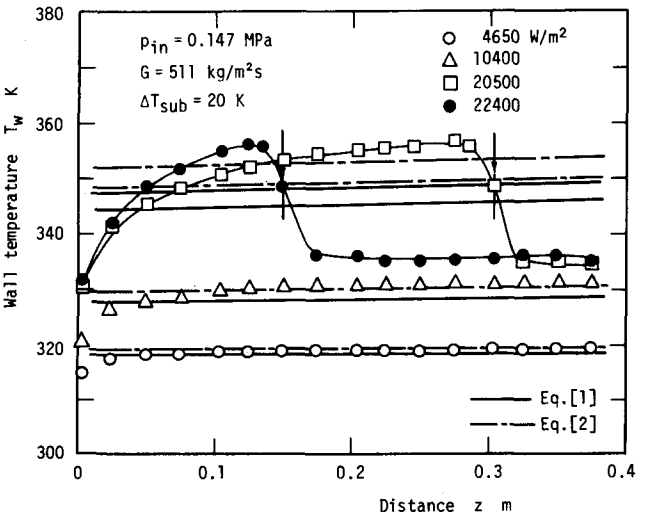

Figure 3. Wall temperature profiles.

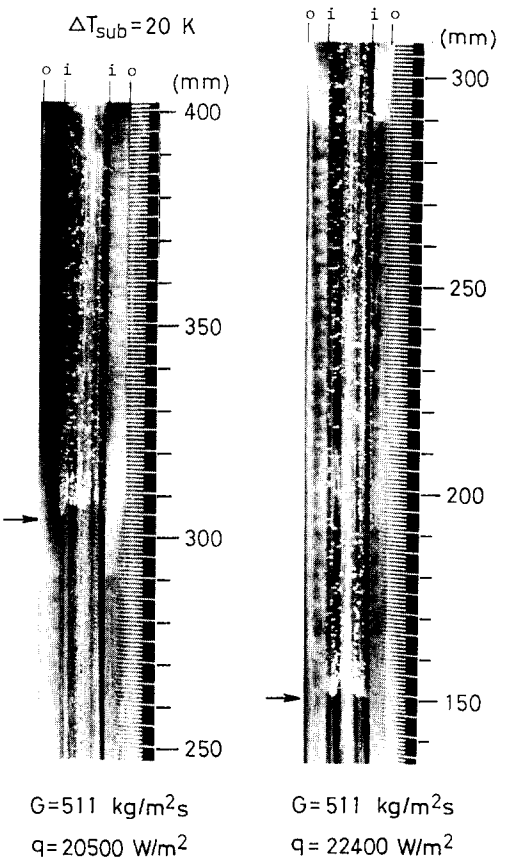

Figure 4. States of the incipient boiling. (lines marked by i and o indicate the positions of inner and outer walls of the test section).

the following well known equations for developed single-phase turbulent flow:

$$qD_e/k_L(T_w - T_L) = 0.023\,(GD_e/\mu_L)^{0.8}\,Pr_L^{0.4}, \quad [1]$$

$$qD_e/k_L(T_w - T_L) = 0.023\,(GD_e/\mu_L)^{0.8}\,Pr_L^{1/3}, \quad [2]$$

where q is the heat flux, T_w and T_L are the wall and liquid temperatures, and k_L and μ_L denote the thermal conductivity and viscosity of the liquid, respectively. Comparison of experimental values with those lines indicates that the liquid flow reaches the developed state at about $z/D_e = 10$.

Figure 4 shows the states of bubble generation corresponding to figure 3. The bubbles were first observed at the position marked by an arrow. This position locates slightly downstream of the starting point of the sharp drop in wall temperature. However, the bubbles first generated on the heated surface are thought to be extremely small and not possible to observe until those grow up to a certain size. Therefore, the start point of the sharp drop in wall temperature is regarded as the actual position of incipient boiling. The bubbles observed move downstream sliding on the heated surface. Size of these bubbles ranges up to 1 mm, and a trend is observed to decrease the average size with increasing liquid flow rate.

3.2 *Incipient boiling condition*

Consider the relation between the heat flux q_{inc} and the wall superheat ΔT_s at the start point of the sharp drop in wall temperature. There are many studies on the incipient boiling condition in forced flow systems. Sato & Matsumura (1964), Bergles & Rohsenow (1964) and Rohsenow (1972) have proposed the following equation for the incipient boiling

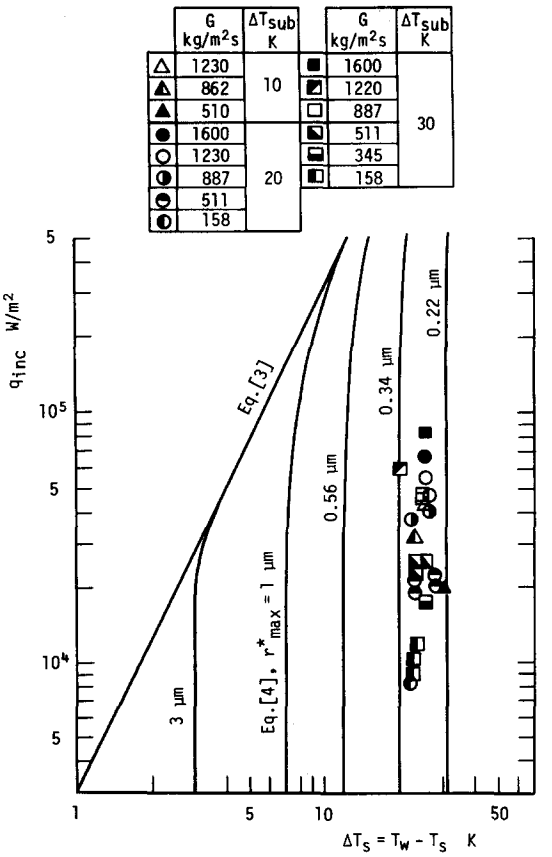

Figure 5. Relation between heat flux and wall superheat at the position of incipient boiling.

condition in the case of the surface cavities of all sizes are available for nucleation:

$$q_{\text{inc}} = \frac{k_L H_{fg} \rho_G}{8 \sigma T_s} (T_w - T_s)^2_{\text{inc}}, \qquad [3]$$

where H_{fg}, ρ_G, σ and T_s are the latent heat of evaporation, vapor density, surface tension and saturation temperature, respectively. In the case where the upper limit of available cavity

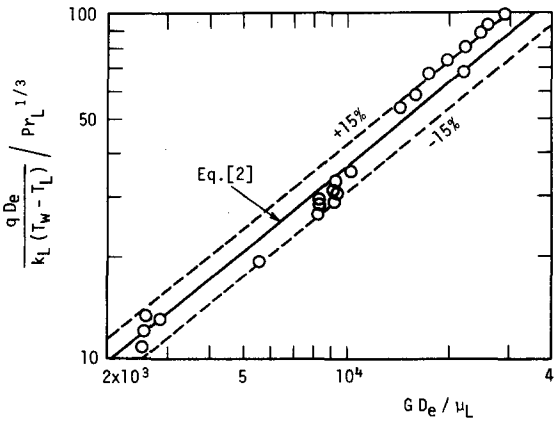

Figure 6. Heat transfer coefficients at the position of incipient boiling.

sizes is restricted to radius r^*_{max}, the incipient boiling condition is expressed as follows:

$$q_{inc} = \frac{k_L}{r^*_{max}}(T_w - T_s)_{inc} - \frac{2\sigma k_L T_s}{H_{fg}\rho_G (r^*_{max})^2}. \quad [4]$$

Figure 5 shows the relation between the heat flux and the wall superheat at the position of incipient boiling obtained from such data as the position locates in the developed flow region of $z/D_e \geq 10$. The lines shown in this figure represent the values of [3] and [4]. The wall superheats obtained in this experiment are much greater than those predicted from [3], and correspond to the case where the available cavity size is limited. The largest radius r^*_{max} ranges from 0.22 to 0.34 μm. This result shows that the wall superheat at the position of incipient boiling is practically independent of the mass velocity and the inlet subcooling.

Figure 6 shows comparison of the heat transfer coefficient at the position of incipient boiling with that calculated from [2]. The present data are in good agreement with [2]. Therefore, when the value of r^*_{max} is known, the heat flux required for incipient boiling at a given location can be predicted from [2] and [4].

3.3 *Boiling curve hysteresis*

It is well known that the boiling curve hysteresis appears in the past history of wall temperature readings for complete cycles of increasing followed by decreasing heat flux.

Figure 7 shows the variation of the wall temperature profile obtained with decreasing heat flux from a state of the incipient boiling is taking place. Arrows drawn in this figure show the position where bubbles were first observed in this test. Observation of the flow state shows that the position remains unchanged until the heat flux decreases to a considerably low value, although the nucleation site density and the bubble number decrease with decreasing heat flux. In this case, the nucleate boiling was terminated completely at q = 10,200 W/m^2.

Figures 8 and 9 show the relation between the heat flux q and the wall superheat ΔT_s obtained at $z/D_e = 35$. In the process to increase the heat flux, the partial nucleate boiling takes place after the incipient boiling characterized by the sharp drop in wall superheat, and then the boiling state moves to the fully developed nucleate boiling with a further increase in heat flux. In the subsequent process to decrease the heat flux, the boiling process turns back along the same curve as the above process in the high heat flux region. However, the

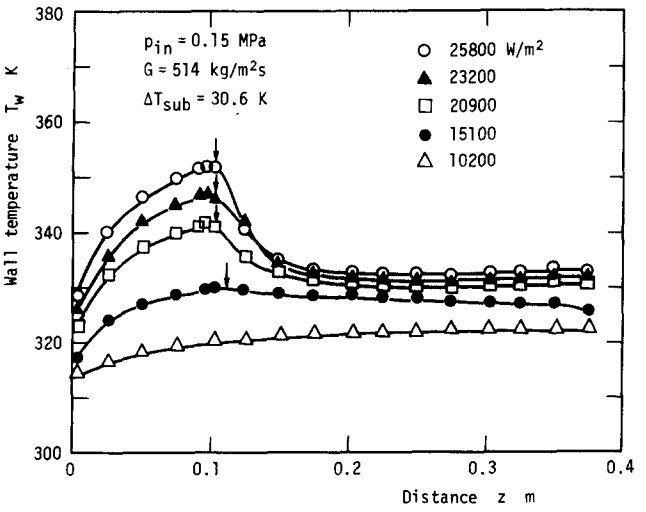

Figure 7. Variation of wall temperature profile with decreasing heat flux.

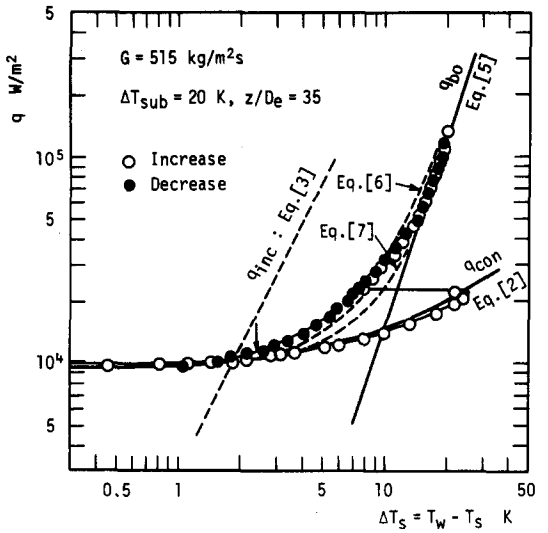

Figure 8. Boiling curve hysteresis.

transition from the partial nucleate boiling to the single-phase forced convective heat transfer does not occur at the heat flux where the nucleate boiling was initiated during the process of heat flux increasing, and the nucleate boiling is maintained until the heat flux decreases to a value near the intersection of this boiling curve and the q_{inc} line calculated from [3]. An arrow marked in this figure indicates the point at which the nucleate boiling was terminated. This sequence of events is considered to be caused by activating large surface cavities of a wide size range during the proceeded intensive boiling.

As a procedure for activating the initially inactive cavities, we may consider the vapor-trapping mechanism suggested by Corty & Foust (1958) and Murphy & Bergles (1972). That is, a first bubble generated on the heated surface covers neighboring large inactive cavities as it grows, and activates them by evaporating the liquid contained in the cavities into the growing bubble. Abdelmessih *et al.* (1972) have observed the bubble behavior by means of high speed cine films, and shown that boiling bubbles growing further begin to slide along the heated surface attaching to it and then depart from the heated

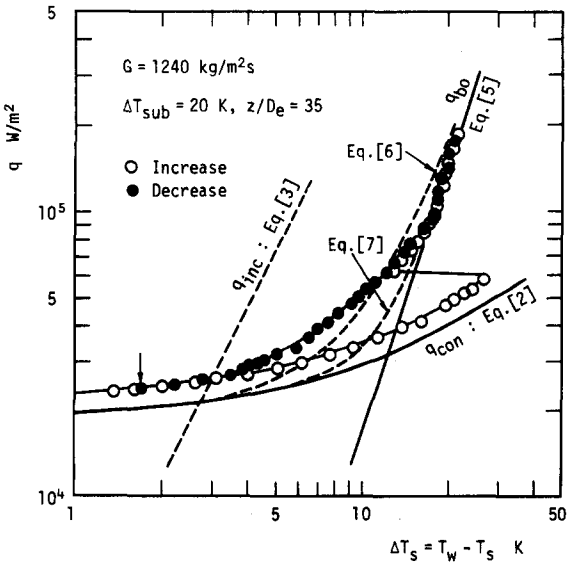

Figure 9. Boiling curve hysteresis.

surface after they grow to a certain size. Therefore, it seems to be that some of initially inactive cavities are activated by the vapor-trapping mechanism during the period of not only the bubble grows at the inherent nucleation site but also the bubble slides along the heated surface.

The line of q_{con} drawn in figures 8 and 9 represents the heat flux for forced convective flow calculated from [2]. The line of q_{bo} represents the heat flux for the fully developed pool boiling obtained from the following Rohsenow's equation (1952):

$$\frac{c_{pL}(T_w - T_s)}{H_{fg}} = C_{sf}\left[\frac{q_{bo}}{\mu_L H_{fg}}\sqrt{\frac{\sigma}{g(\rho_L - \rho_G)}}\right]^{0.33} Pr_L^{1.7}, \quad [5]$$

where $C_{sf} = 0.006$ is assumed to fit the present data. In the partial nucleate boiling region of low nucleation site densities, the heat transfer characteristic can be determined by combining effects of forced convection and nucleate boiling. For this region, Clark & Rohsenow (1954) have assumed the following equation:

$$q = q_{con} + q_{bo} \quad [6]$$

and Bergles & Rohsenow (1964) suggested the following correlation:

$$q = q_{con}\left[1 + \left\{\frac{q_{bo}}{q_{con}}\left(1 - \frac{q_{bi}}{q_{bo}}\right)\right\}^2\right]^{1/2}. \quad [7]$$

Here, q_{bi} represents the heat flux obtained by substituting the wall superheat at the intersection of the curves [2] and [3] into [5]. Dotted lines in figures 8 and 9 represent the boiling curves for the partial nucleate boiling region calculated from [6] to [7] by applying q_{con} and q_{bo} mentioned above. The present data are close to the prediction of [6].

4. POINT OF NET VAPOR GENERATION AND FULLY DEVELOPED NUCLEATE BOILING

4.1 *Point of net vapor generation*

With increasing heat flux, the position of incipient boiling shifts upstream, and a bubbly layer is formed along the heated length. Then, relatively large bubbles begin to depart from the bubbly layer at a certain position along the heated length, and a rapid increase in void fraction is initiated. This position characterized by the sharp increase in void fraction is generally called as the point of net vapor generation.

Figure 10 shows typical flow states around the point of net vapor generation. This flow state is similar to that observed by Sekoguchi *et al.* (1975) for the air–water two phase flow arranged to simulate the flow boiling. In the region I of subcooled boiling flow, the bubbly layer consists of growing bubbles and sliding bubbles. The bubble density in the bubbly layer increases along the heated length, and then relatively large bubbles grown up in the layer begin to depart from the heated surface. However, the photographs indicate that, even in the low bubble density bubbly layer in the region I, a few minute bubbles are departed into the liquid core.

Then, by examining 9–15 photographs taken for each heat flux, the point of net vapor generation was determined on the following conditions:

(1) Bubbles cover densely the whole heated surface periphery.

(2) Bubbles are grown up fairly on the heated surface. Here, the bubble which is not less than 1 mm in width is regarded as the grown up one.

(3) The grown up bubbles are continuously departing from the bubbly layer.

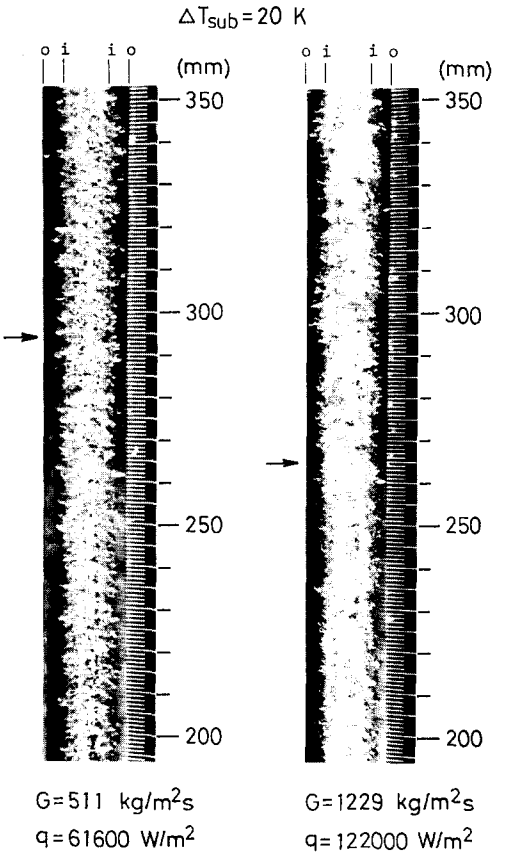

Figure 10. Flow states around the point of net vapor generation.

The position shown by an arrow in figure 10 represents the point of net vapor generation determined by the above conditons.

Data of local subcooling, $\Delta T_B = T_s - T_{LB}$, at the point of net vapor generation thus derived are compared with the correlation of Saha & Zuber (1974). Figure 11 shows the result where the solid line represents the Saha's correlation given by

$$Pe \leq 70{,}000, \quad Nu_B = \frac{q\, D_e}{k_L\, \Delta T_B} = 455,$$
$$Pe > 70{,}000, \quad St_B = \frac{q}{G\, c_{pL}\, \Delta T_B} = 0.0065. \qquad [8]$$

The present data are in good agreement with [8].

Considering a force balance exerted on the bubble in contact with wall, Levy (1967) has proposed the following equation for the bubble height at the point of net vapor generation:

$$y_b = 0.015 \left(\frac{\sigma\, D_e}{\tau_w}\right)^{1/2}, \qquad [9]$$

where τ_w denotes the wall shear stress. The frictional pressure drop gradient $(\Delta p/\Delta z)_F$ for single-phase liquid flow can be expressed as

$$\left(\frac{\Delta p}{\Delta z}\right)_F = \frac{4f}{D_e}\frac{G^2}{2\,\rho_L}. \qquad [10]$$

The friction factor derived from the measured pressure drop for single-phase liquid flow in

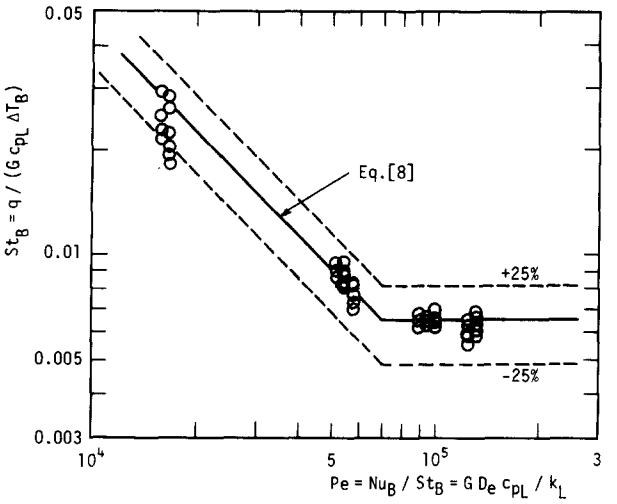

Figure 11. Correlation of the point of net vapor generation.

the present test section was well correlated by

$$f = 0.051 \left(\frac{GD_e}{\mu_L}\right)^{-0.25}. \qquad [11]$$

Then, for reference, the bubble height y_b of [9] was estimated by applying the wall shear stress calculated from $\tau_w = fG^2/(2\rho_L)$. The values of y_b thus derived under the inlet subcooling ΔT_{sub} = 10–30 K were $y_b \approx 0.27$ mm for $G = 514$ kg/m^2 s and $y_b \approx 0.13$ mm for $G = 1236$ kg/m^2 s. These values are remarkably lower than the bubble diameters observed at the point of net vapor generation.

4.2 *Fully developed boiling region*

Figures 12 and 13 show the boiling curves up to the CHF condition obtained at the position of $z/D_e = 35$. In these figures, solid arrows indicate the point of net vapor generation calculated from [8] and dotted arrows indicate the CHF, i.e. the heat flux just before the sharp rise in wall temperature. These figures suggest that the point of net vapor generation locates near the transition point from the partial nucleate boiling to the fully developed nucleate boiling. Therefore, it is considered that the region I of the subcooled boiling flow corresponds approximately to the partial boiling region and the region II to the fully developed boiling region.

As mentioned before, it was observed that a few minute bubbles departed from the bubbly layer under flow states of the region I. Dougall & Lippert [1971] determined the condition under which departed bubbles were first observed in the liquid core by taking photographs of R-113 subcooled boiling flow, and indicated that the condition corresponded to the intersection of the boiling curve in the partial nucleate boiling region and a line given by the following equation:

$$\begin{aligned} q_b &= Sq_{bo}, \\ S &= 1 + 0.0417\,[c_{pL}\,\Delta T_{sub}/H_{fg}]^{-1.432}, \end{aligned} \qquad [12]$$

where q_{bo} is the heat flux in the fully developed nucleate boiling region obtained by [5]. Dotted lines shown in figures 12 and 13 are the value of [12]. Photographic observation in the present experiment shows that a few minute bubbles depart from the bubbly layer under the condition near the intersection point in these figures. However, since these bubbles

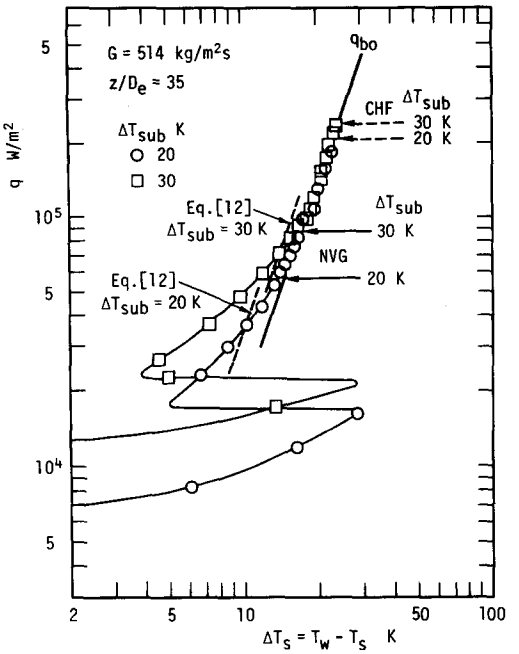

Figure 12. Boiling curves.

condense in the liquid core immediately, they do not contribute much to increase the void fraction. Therefore, it seems to be that this intersection can not be regarded as the point of net vapor generation.

From the observation of flow states, it is shown that the bubble density on the heated surface increases with increasing heat flux, and that remarkably large bubbles yielded by coalescence of bubbles appear close to the heated surface. Figure 14 is the flow states observed near the CHF condition. The coalescent bubbles are considered to be related closely to the occurrence of the CHF condition. However, as is seen in figure 14, it was difficult to distinguish qualitatively the flow state close to the heated surface from the bubbles flowing in the core. For investigating the flow state adjacent to the heated surface, the other measurements will be needed. For this purpose, the distributions of temperature and its

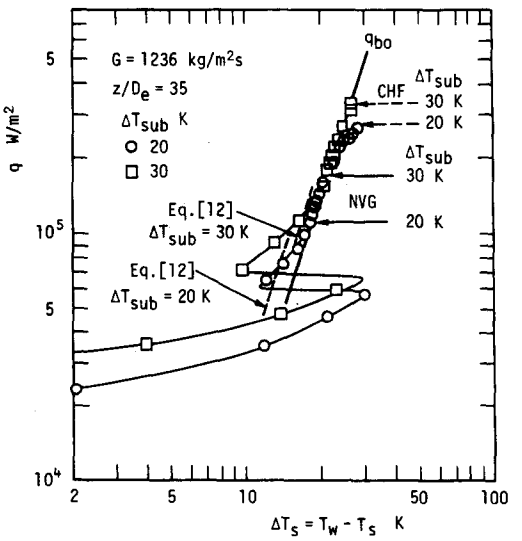

Figure 13. Boiling curves.

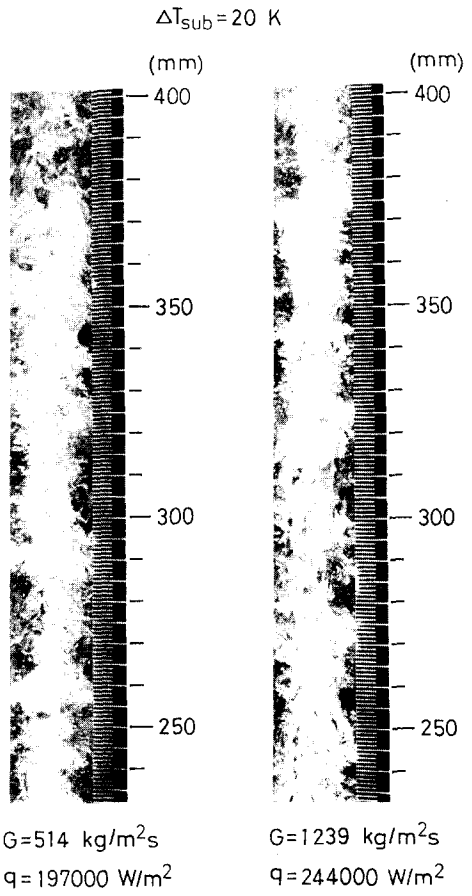

Figure 14. Flow states near the CHF condition.

fluctuation in the flow adjacent to the heated surface are measured, the results will be presented in the following paper, part 2.

5. CONCLUSIONS

The wall temperature measurement and the photographic observation were performed on the R-113 upward subcooled boiling flow in an annulus with a uniformly heated inner tube. From the results, the following conclusions were obtained.

(1) The wall superheat at the position of incipient boiling is relatively high and a sharp drop in wall temperature takes place by the boiling initiation. The incipient boiling corresponds to the case where the upper limit of available cavity sizes is restricted. In this experiment, the largest available cavity radius, r^*_{max}, ranges from 0.22 to 0.34 μm. The wall superheats at the incipient boiling position are practically independent of the mass velocity and the inlet subcooling.

(2) The boiling curve hysteresis is considered to be a result of the activation of relatively large cavities by the proceeded intensive boiling.

(3) The results of the point of net vapor generation determined by photographic observation are in good agreement with the correlation given by Saha & Zuber. This point locates near the transition point from the partial nucleate boiling to the fully developed nucleate boiling on the boiling curve.

(4) Increasing heat flux to the critical heat flux, remarkably large coalescent bubbles appear near the exit end of the heating section periodically.

Acknowledgement—The authors gratefully acknowledge the support for this work by the research fund (Grant in Aid of Energy Special Project Research) of the Ministry of Education, Japan.

REFERENCES

ABDELMESSIH, A. H., FAKHRI, A. & YIN, S. T. 1974 Hysteresis effects in incipient boiling superheat of freon 11. *Proc. 5th Int. Heat Transfer Conf., Tokyo* **4,** 165–169.

ABDELMESSIH, A. H., HOOPER, F. C. & NANGIA, S. 1972 Flow effects on bubble growth and collapse in surface boiling, *Int. J. Heat Mass Transfer* **15,** 115–125.

BERGLES, A. E. & ROHSENOW, W. M. 1964 The determination of forced-convection surface boiling heat transfer. *Trans. ASME, Ser. C* **86,** 365–372.

CLARK, J. A. & ROHSENOW, W. M. 1954 Local boiling heat transfer to water at low Reynolds numbers and high pressures. *Trans. ASME* **76,** 553–563.

CORTY, C. & FOUST, A. S. 1958 Surface variables in nucleate boiling. *Chem. Eng. Progr. Symp. Ser. No. 17,* 1–12.

DAVIS, E. J. & ANDERSON, G. H. 1966 The incipience of nucleate boiling in forced convection flow. *AIChE. J.* **12,** 774–780.

DOUGALL, R. S. & LIPPERT, T. E. 1971 Net vapor generation point in boiling flow of trichlorotrifluoroethane at high pressures, NASA Rep., CR-2241.

LEVY, S. 1967 Forced convection subcooled boiling—prediction of vapor volumetric fraction. *Int. J. Heat Mass Transfer* **10,** 951–965.

MURPHY, R. W. & BERGLES, A. E. 1972 Subcooled flow boiling of fluorocarbons—hysteresis and dissolved gas effects on heat transfer. *Proc. 1972 Heat Transfer and Fluid Mechanics Institute,* 400–416, Stanford Univ. Press.

ROHSENOW, W. M. 1972 Status of and problems in boiling and condensation heat transfer. *Progress in Heat and Mass Transfer* **6,** 1–44.

ROHSENOW, W. M. 1952 A method of correlating heat-transfer data for surface boiling of liquids, *Trans. ASME* **74,** 969–976.

SAHA, P. & ZUBER, N. 1974 Point of net vapor generation and vapor void fraction in subcooled boiling. *Proc. 5th Int. Heat Transfer Conf., Tokyo* **4,** 175–179.

SATO, T. & MATSUMURA, H. 1964 On the conditions of incipient subcooled-boiling with forced convection. *Bull. Jpn. Soc. Mech. Engr.* **7,** 392–398.

SEKOGUCHI, K., NISHIKAWA, K., NAKASATOMI, M., HIRATA, N. & HIGUCHI, H. 1974 Flow boiling in subcooled and low quality regions—heat transfer and local void fraction. *Proc. 5th Int. Heat Transfer Conf., Tokyo* **4,** 180–184.

SEKOGUCHI, K., KAWAKAMI, Y. & NISHIKAWA, K. 1975 Simulation of forced-flow boiling with air–water two phase fluids. *Trans. Jpn. Soc. Mech. Engr.* **41,** 1889–1898.

STAUB, F. W. 1968 The void fraction in subcooled boiling—prediction of the initial point of net vapor generation, *Trans. ASME, Ser. C* **90,** 151–157.